

Supporting Information

Designing Jasmine Lactone Copolymer Micelles for Drug Delivery: Influence of Ionic Group Density and Chain Length

Vishal Kumar,^{a,b} Elisa Léonard,^{a,b#} Atefeh Atefi,^{a,c} Jessica M. Rosenholm,^a Carl-Eric Wilén,^b Shakhawath Hossain,^{d*}, Kuldeep K. Bansal.^{a,b*}

^a*Pharmaceutical Sciences Laboratory, Faculty of Science and Engineering Åbo Akademi University, Biocity, Tykistökatu 6A, 20520 Turku, Finland.*

^b*Laboratory of Molecular Science and Engineering, Faculty of Science and Engineering, Åbo Akademi University, Aurum, Henrikinkatu 2, 20500 Turku, Finland.*

^c*Faculty of Science and Engineering, Cell Biology, Åbo Akademi University, Biocity, Tykistökatu 6A, 20520 Turku, Finland.*

^d*Department of Pharmacy and The Swedish Drug Delivery Center (SweDeliver), Uppsala University, Uppsala 751 23, Sweden.*

*corresponding authors, E-mail address: shakhawath.hossain@uu.se, kuldeep.bansal@abo.fi,

#Present address: Department of chemistry, Toulouse INP, ENSIACET 4 allee, Emile Monso, 31030 Toulouse France.

Table of content:

1. Material:.....	3
2. Methods:	3
2.1 Synthesis of block copolymer (mPEG-b-PJL) of jasmine lactone.....	3
2.2 Functionalization of block copolymer (mPEG-b-PJL) into mPEG-b-PJL-COOH.	4
2.3 Assessment of critical micelles concentration (CMC).....	6
2.4 Aqueous Solubility of TMP and Chlorine e6.	6
2.5 Preparation of TMP (TMP) chlorine e6 (Ce6) loaded and blank micelles.	7
2.6 In vitro drug release.....	7
2.7 In vitro cytotoxicity of blank micelles.....	7
2.8 Ex vivo haemolytic study of blank micelles.....	8
2.9 Statistical analysis.	8
3. Instruments and characterization:	9
3.1 Characterization of the synthesized polymers.	9
3.2 Characterization of drug loaded and blank micelles.....	9
4. Coarse-grained molecular dynamics (MD) simulations:	10
4.1 Generation of coarse-grained structures and topologies.	10
4.2 Coarse-grained simulation details.....	14
4.3 All-atom simulation details.	14
4.4 Umbrella sampling (US) simulations for the TMP logP calculation.	14
5. Simulation analysis:.....	15
6. Results-supporting Figures:	16
7. References:	32

1. Material:

Jasmine lactone ($\geq 97\%$) was purchased from Lluch Essence, Spain. Poly (ethylene glycol) methyl ether (mPEG, Mn = 5.0 kDa), 1,5,7-triazabicyclo [4.4.0]dec-5- ene (TBD) (98%), mercaptopropionic acid (99%), 11-mercaptopoundecanoic acid (98%), dimethoxy-2-phenylacetophenone (99%) (DMPA), sodium chloride, triton X-100, HPLC grades methanol ($\geq 99.9\%$), acetone ($\geq 99.8\%$), deuterated dimethyl sulfoxide (DMSO-d₆), deuterated chloroform (CDCl₃), di ethyl ether (DEE), petroleum ether (PE) tetrahydrofuran, Fetal Bovine Serum (FBS), trypsin, and dimethyl sulfoxide (DMSO) were purchased from Sigma-Aldrich, Finland. Trimethoprim (TMP) was purchased from Apolo scientific and Chlorine e6 (Ce6) was from the Cayman chemical company. Dialysis membrane tubing was purchased from the spectrum laboratories Canada. Phosphate buffered saline (PBS) and DMEM high glucose were purchased from Euroclone, Italy and Alamar Blue was purchased from TCI Europe.

2. Methods:

2.1 Synthesis of block copolymer (mPEG-b-PJL) of jasmine lactone.

In this study, two different chain length copolymers, polymer A (PA) and polymer B (PB) of jasmine lactone (mPEG-b-PJL), were synthesized by ring-opening polymerization (scheme S1) following the reported procedure¹. For the synthesis of the PA, 19.99 g (118.8 mmol) of jasmine lactone monomer and 20 g (4 mmol) of mPEG5K as an initiator were weighed in 100 ml of RBF and a glass beaker, respectively, while the catalyst TBD 0.41 g (2.97 mmol) was weighed in a glass vial, and the traces of the moisture were removed by keeping them under vacuum for 2 nights at room temperature. Later, in a nitrogen environment, mPEG5K was added to the RBF containing jasmine lactone and stirred for 10 minutes at 50°C, and TBD was then added into the transparent homogeneous mixture to start the reaction. The progress of the reaction was monitored by ¹H NMR spectroscopy, and after 54% conversion, the reaction mixture was quenched by adding an excess of benzoic acid in acetone. The pure polymer was obtained by precipitating the reaction mixture twice in cold methanol and twice in diethyl ether, followed by drying under vacuum. The similar procedure with a different degree of polymerization was followed to synthesize the PB, where 10.7 g (64 mmol) of jasmine lactone, 4 g (0.8 mmol) of mPEG, and 0.22 g (1.6 mmol) of TBD were used, and the pure polymer was obtained after 70% conversion followed by a similar purification method.

¹H NMR details of PA- (500 MHz, CDCl₃) δ 5.52 – 5.41 (m, 14H), 5.32-5.20 (m, 15H), 4.93 – 4.80 (m, 15H), 4.21 (t, 2H), 4.03 (s, 1H), 3.63 (s, 627H), 3.36 (s, 3H), 2.36 – 2.19 (m, 65), 2.10 – 1.96 (m, 32H), 1.72 – 1.40 (m, 65H), 0.96 (t, 50H).

Calculated mol. weight by ^1H NMR - 7.5kDa

Mol. Weight (Mn) by SEC- 6.0kDa, Polydispersity index (D)1.8

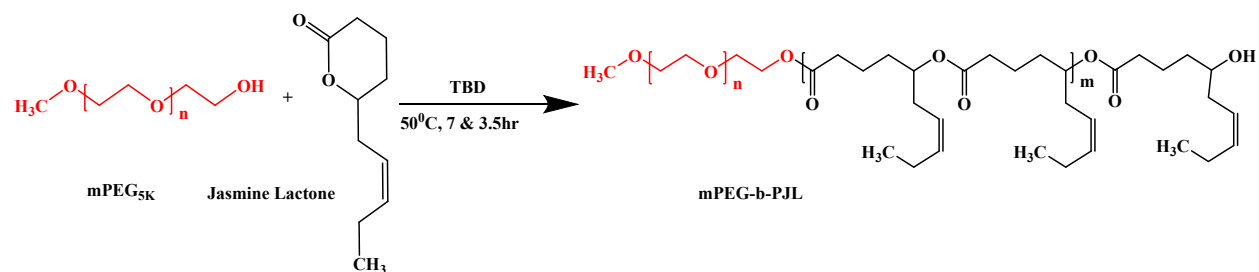
Yield- 18g

^1H NMR details of PB- ^1H NMR (500 MHz, CDCl_3) δ 5.52 – 5.40 (m, 46H), 5.33 – 5.20 (m, 47H), 4.91 (m 47H), 4.24 (t, 2H), 4.04 (s, 1H), 3.63 (s, 600H), 3.37 (s, 3H), 2.37 – 2.19 (m, 188H), 2.08 – 1.97 (m, 94H), 1.71 – 1.48 (m, 179H), 0.95 (t, 144H).

Calculated mol. weight by ^1H NMR - 12.9kDa

Mol. Weight (Mn) by SEC- 16.3kDa, Polydispersity index (D)1.1

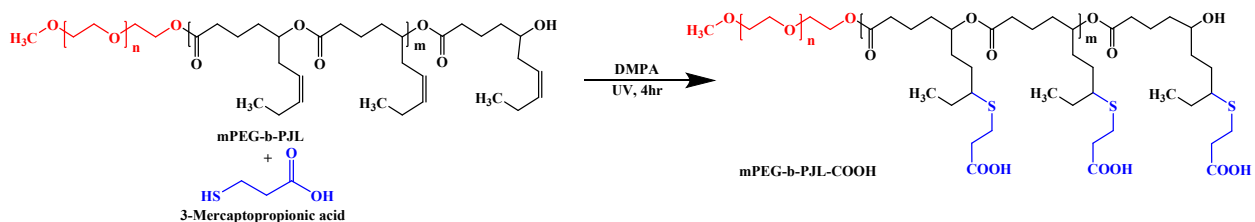
Yield- 7g



Scheme S1. Ring opening polymerization of jasmine lactone. TBD (1,5,7-triazabicyclo [4.4.0] dec-5- ene). 7hr for polymer A and 3.5hr for Polymer B.

2.2 Functionalization of block copolymer (mPEG-b-PJL) into mPEG-b-PJL-COOH.

To check the effect of acid (-COOH) groups on drug loading, release, and cytotoxicity, the above-synthesized block copolymer (mPEG-b-PJL) PB was functionalized to its acid derivatives (mPEG-b-PJL-COOH) by thiol-ene click reaction (scheme S2) having different numbers of the COOH groups (acronyms P2 and P3) by following the reported procedure¹. In brief, for the P2, 2.25 g (1.7 mmol) of PB and 0.045 g (1.2 mmol) of dimethoxy phenyl acetophenone (DMPA), while for the P3, 0.8 g (0.06 mmol) of PB and 0.16 g (5.8 mmol) of DMPA were dissolved in a sufficient quantity of tetrahydrofuran (THF), then this mixture was added into an RBF containing 2.4 g (23 mmol) and 0.94 g (8.8 mmol) of 3-mercaptopropionic acid (3-MPA) for P2 and P3, respectively. The RBF was placed under a UV cabinet fitted with a blacklight 368 nm lamp (15W, Sylvania) and continued to stir at room temperature. After 4 h of stirring, the THF was evaporated, and pure polymers were obtained by precipitation in cold diethyl ether (DEE).



Scheme S2. Thiol ene click reaction to functionalize the mPEG-b-PJL into mPEG-b-PJL-COOH with 3-mercaptopropionic acid. DMPA (di methoxy phenyl acetophenone), UV (ultraviolet).

¹H NMR details of P2- (500 MHz, CDCl₃) δ 5.57 – 5.49 (m, 15H), δ 5.45 – 5.30 (m, 15H), 5.29 – 5.24 (m, 46H), 4.27 – 4.16 (t, 2H), 4.06 (s, 1H), 3.67 (s, 625H), 3.37 (s, 3H), 3.21 – 2.57 (m, 159H), 2.27- 2.50 (m, 100H), 2.00 (m, 31H), 1.90 – 1.30 (m, 409H), 1.12 – 0.83 (m, 141H).

Calculated mol. weight by ¹H NMR - 16.2kDa

Mol. Weight (Mn) by SEC- 14.8kDa, Polydispersity index (D)-2.2
Yield- 2.3g

¹H NMR details of P3- (500 MHz, CDCl₃) δ 5.48 - 4.81 (m, 46H), 4.27 – 4.22 (m, 2H), 4.08 (s, 1H), 3.67 (s, 628H), 3.39 (s, 3H), 3.21 – 2.57 (m, 232H), 2.35 (m, 90H), 1.95 – 1.40 (m, 460H), 1.10 – 0.90 (m, 142H).

Calculated mol. weight by ¹H NMR - 16.4kDa

Mol. Weight (Mn) by SEC- 17.5kDa, Polydispersity index (D)-1.4
Yield- 0.81g

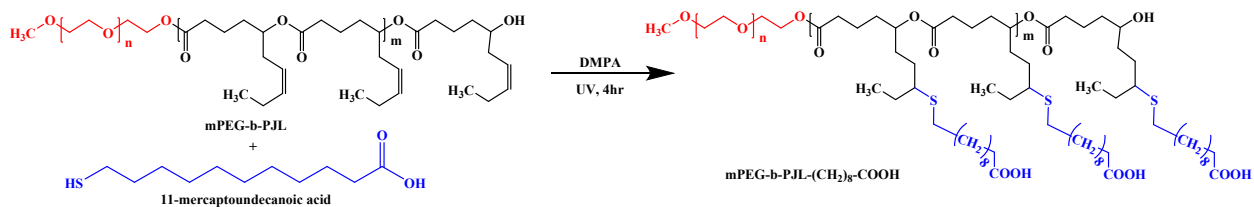
Additionally, a long-chain hydrocarbon acid was utilized for functionalization of PA to its carboxylic acid derivative (mPEG-b-PJL-COOH) (acronym P4) by using 11-mercaptoundecanoic acid (11-MUDA) (scheme S3). The method of functionalization remains the same as above. Briefly, 1 g (0.13 mmol) of PA and 0.24 g (0.95 mmol) of DMPA were dissolved in 3 ml of THF and added into an RBF containing 1.25 g (5.72 mmol) of 11-mercaptoundecanoic acid (11-MUDA) and stirred in a UV cabinet fitted with a blacklight 368 nm lamp (15 W, Sylvania). After 4 h of stirring, the THF was evaporated, and the pure polymer was obtained by washing in a cold mixture (60:40) of diethyl ether and petroleum ether.

¹H NMR details of P4- (500 MHz, CDCl₃) δ 5.57 – 5.49 (m, 1H), δ 5.45 – 5.30 (m, 1H), 5.29 – 5.24 (m, 13H), 4.27 – 4.16 (t, 2H), 4.06 (s, 1H), 3.63 (s, 633H), 3.37 (s, 3H), 2.63-2.23 (m, 94H), 2.04 – 1.95 (m, 2H), 1.78 – 1.20 (m, 346H), 1.07 – 0.82 (m, 41H).

Calculated mol. weight by ¹H NMR - 9.8kDa

Mol. Weight (Mn) by SEC- 13.8kDa, Polydispersity index (D)2.4.

Yield- 1.05g



Scheme S3. Thiol ene click reaction to functionalize mPEG-b-PJL to produce mPEG-b-PJL-(CH₂)₈-COOH using 11-mercaptoundecanoic acid. DMPA (dimethoxy-2-phenylacetophenone).

2.3 Assessment of critical micelles concentration (CMC).

The CMC of functionalized polymers (P2, P3, and P4) was assessed by applying reported method¹. In brief, a stock (6.10⁻⁷ M) solution of pyrene in acetone was prepared, and a precise volume with calculated concentration was transferred to different vials, and the acetone was evaporated by keeping the vials in the dark at room temperature under a slow flow of nitrogen. The solution of polymers in water with the concentration range (from 0.001 to 200 µg/mL) was added to vials and left overnight in the dark under agitation to equilibrate. After 24 h, fluorescence spectra of each solution were measured in the range of 350 to 420 nm with an excitation wavelength of 335 nm on a PC1 photon counting spectrofluorometer. The intensities of the fluorescence light emitted at 376 nm (I₁) and 393 nm (I₃) are plotted against the log concentration of the polymers. The obtained graph was fitted using nonlinear regression (sigmoidal, 4PL, X-axis log scale) to determine the CMC value. The inflection point (IC) of the sigmoidal curve was considered the CMC value of the polymer.

2.4 Aqueous Solubility of TMP and Chlorine e6.

Maximum aqueous solubility of the TMP and Ce6 was determined by following the reported saturation shake-flask method with slight modification². In brief, an excess quantity of the drug was added to a 4 ml glass vial containing 1 ml of DI water, capped, and continued to stir at ambient temperature for 48 hr in a light-protected environment. After that the samples were centrifuged at 13.5k RPM for 7 minutes (Microcentrifuge Scanspeed, Labogene, Lyngé, Denmark), filtered using a 0.45 µm polypropylene membrane syringe filter, and the soluble drug was quantified using UV spectroscopy.

2.5 Preparation of TMP (TMP) chlorine e6 (Ce6) loaded and blank micelles.

To assess the effect of the anionic groups on drug loading, a basic drug, TMP, and an acidic photosensitizer molecule, Ce6, loaded polymeric micelles (P1-M, P2-M, P3-M, and P4-M) of the polymers (P1, P2, P3, and P4) were prepared via the reported nanoprecipitation method³. In short, 20 mg of the respective polymer, 3 mg of TMP, and 2 mg of Ce6 were dissolved in the 1 ml of methanol (organic phase), and this organic phase was added dropwise to the 1 ml of DI water (aqueous phase) in a 4 ml glass vial preplaced on a magnetic stirrer stirring (700 rpm) and continued to stir for approximately two days for the complete removal of the organic phase. Any untrapped drug was later removed by centrifugation at 13.5k RPM for 7 minutes (Microcentrifuge Scanspeed, Labogene, Lynge, Denmark) followed by filtration through a 0.45 μ m polypropylene membrane syringe filter and stored at 4°C for further characterizations. Similarly, the blank micelles of each polymer were prepared at 20 mg/ml concentration and characterized for size by the DLS technique.

2.6 In vitro drug release.

The release profile of free TMP, free Ce6, and their micellar formulations were performed using the reported procedure with slight modification⁴. Briefly, a known quantity of the free drug dissolved in the 1:1 (DI water and methanol) and micelles with a calculated concentration of TMP and Ce6 were diluted up to 3 mL in DI water and placed in pre-wetted membrane tubing (SpectraPor®) with the molecular weight cut-off (MWCO) of 6 to 8 kDa. Then these tubes were placed in a glass beaker containing 30 ml and 500 ml of the PBS (pH 7.2) for TMP and Ce6, respectively, and kept in a water bath at 37°C with gentle shaking. To measure the TMP drug release, 1 ml of medium was withdrawn for analysis from dissolution media and replaced with preheated (37°C) fresh medium. For the Ce6 analysis, 1 ml of the sample was taken directly from the tube after adjusting the volume up to the mark of tube (if necessary) and the absorbance at 286 nm (TMP) and 661 nm (Ce6) was measured by UV spectroscopy (NanoDrop 2000c from Thermo Fisher Scientific), and the percentage of cumulative drug released was calculated. The samples were taken directly from dialysis tubing in case of Ce6 release study due to its poor solubility in release media and thus more media is needed, which diluted the Ce6 below the detection level.

3.1 In vitro cytotoxicity of blank micelles.

An Alamar blue assay was employed to analyze the cytotoxicity of the synthesized polymeric micelles on the mouse embryonic fibroblast (MEF) and metastatic mammary adenocarcinoma (MDA-MB-231) cells⁵. Briefly, cells were seeded in a 96-well plate at a density of 5000

cells/well in high-glucose Dulbecco's modified Eagle's medium (DMEM) and incubated for 24 h. After 24 h, the media was replaced with the blank micelles diluted at varying concentrations (0.25, 0.5, 0.75, and 1 mg/mL) in cell culture medium, and then the plates were incubated further at 37°C (5% CO₂) for 48 h. After incubation, 10 µl of Alamar Blue cell proliferation reagent was added to each well and further incubated for 3 h, followed by measurement of fluorescence intensity with an excitation wavelength of 540 nm and emission between 560 and 590 nm. The percentage of cell proliferation was determined by comparing the fluorescence of cells exposed to micelles with that of cells grown in untreated culture medium (considered as 100% viability).

2.8 Ex vivo haemolytic study of blank micelles.

The biocompatibility and pH-dependent cell membrane disruption potential of the anionic functionalized polymers was assessed following the reported RBCs hemolysis assay on human blood RBCs⁶. For the biocompatibility analysis, the blank micelles of all 4 polymers were prepared in DI water, while to understand the potential to destabilize cell membranes at endosomal pH, micelles were prepared in citrate buffer (100 mmol) of pH 5, 5.5, and 6 at a concentration of 20 mg/ml. The micelles were diluted in the same buffer (intended to be used in the study) to concentrations of 0.5, 1, 5, and 10 mg/mL for the biocompatibility study and 10, 25, 50, and 100 µg/mL for the pH-dependent cell membrane disruption potential. After the dilution of the micelles, the RBCs from anonymous human blood were prepared according to the reported procedure and incubated with the micelles at 37°C (HERA CELL 150i CO₂ Incubator) for 1, 2, and 24 h. After incubation, samples were centrifuged for 2 min at 4K, 200 µl of clear supernatant was added into the 96-well plate, and the absorbance was recorded (Varioskan Flash) at 410 nm. The following formula was used to calculate the % hemolysis.

$$\% \text{hemolysis} = \frac{\text{Abs (sample)} - \text{Abs (negative control)}}{\text{Abs (positive control)} - \text{Abs (negative control)}} \times 100$$

2.9 Statistical analysis.

The data was analyzed using the one-way ANOVA, column analysis (multiple comparisons) followed by Tukey's multiple comparisons test, computed using GraphPad Prism 8.0 software by considering differences as statistically significant at P < 0.05. The values of data are presented as the mean ± standard deviation of the mean (mean ± STD) of three values.

3. Instruments and characterization:

3.1 Characterization of the synthesized polymers.

The chemical structure and molar mass (M_n) of synthesized polymers were analysed by proton nuclear magnetic resonance (¹H NMR) spectroscopy using a Bruker NMR 500 MHz spectrometer (Bruker, Coventry, United Kingdom). Deuterated chloroform (CDCl₃) was used as a solvent for NMR analysis. The number-average molar mass (M_n), weight-average molar mass (M_w), and mass distribution (polydispersity (D), M_w/M_n) of the synthesized polymers were also determined by size exclusion chromatography. A 2 mg/ml solution of polymers in THF was analyzed by the instrument fitted with a low-temperature evaporative light scattering detector (LT-ELSD) with an AM GEL linear column (10 μ particle size) and an AM gel guard column (300 × 7.8 mm). Column calibration was done using narrow polystyrene standards of known M_n and D in the range of 600–2300 kDa. Tetrahydrofuran (THF) was used as the mobile phase at 40°C with a flow rate of 1 mL/min.

3.2 Characterization of drug loaded and blank micelles.

The maximum drug loading in micelles was measured by the UV-Vis spectrophotometer (NanoDrop 2000c from Thermo Fisher Scientific) after diluting in methanol, and the drug content (DC) and encapsulation efficiency (EE) of the polymers were calculated after the deduction of maximum solubility of the loaded molecule in DI water using the previously published mathematical procedure with the slightly modified formula given below⁷.

$$DC (\%) = \frac{Quantity\ of\ drug\ in\ micelles - Quantity\ of\ free\ drug\#}{Quantity\ of\ micelles} \times 100$$

$$EE (\%) = \frac{Quantity\ of\ drug\ in\ micelles - Quantity\ of\ free\ drug\#}{Quantity\ of\ used\ drug} \times 100$$

maximum solubility of the free drug in solvent.

The size and polydispersity index (PDI) of the TMP-loaded and blank micelles at a polymer concentration of 20 mg/ml, while the Ce6-loaded micelles at a polymer concentration of 1 mg/ml, were analyzed by the dynamic light scattering (DLS) (Malvern Instruments, UK) at 25°C. The shape and size of the micelles was further confirmed by the transmission electron microscope (TEM). The grid containing the samples was stained with a 0.2% solution of uranyl acetate, and images were captured using a JEM 1400-Plus (JEOL Ltd., Tokyo, Japan).

4. Coarse-grained molecular dynamics (MD) simulations:

4.1 Generation of coarse-grained structures and topologies.

Coarse-grained MD simulations were performed using the Martini 3 force field for system⁸ this system contains polymers and drug molecules, as well as systems used to investigate polymer–membrane interactions, as summarized in Table S1.

To generate the coarse-grained structures and topologies for the polymers with varying numbers of PJL-COOH units, we first built all-atom topologies. The structure and topology of the mPEG segment were directly obtained using the Charmm-GUI Polymer Builder⁹. For a single PJL-COOH unit, the all-atom structure was generated using an automated parameterization process via the Charmm General Force Field (CGenFF)¹⁰. This tool provides penalty scores associated with partial charges and torsional angles. Penalty scores below 10 indicate acceptable analogies, while scores between 10 to 50 suggest reasonable analogies that may require further validation. For the PJL-COOH unit, the maximum penalty scores were 5 (for partial charges) and 6.5 (for torsional bonds), indicating satisfactory reliability.

An all-atom mPEG–PJL-COOH model was then constructed with 114 mPEG units, representing a 5K mPEG molecular weight, and 30 PJL-COOH units. All-atom simulations were performed to obtain the necessary bond connectivity and angular distributions-both within and between PJL-COOH units, as well as between mPEG and PJL-COOH segments. These parameters were used to define the coarse-grained beads and construct the coarse-grained topology. The coarse-grained representation of PJL-COOH units, along with comparisons of bond lengths and angles between all-atom and coarse-grained simulations, is shown in Fig. 1 and 2, respectively.

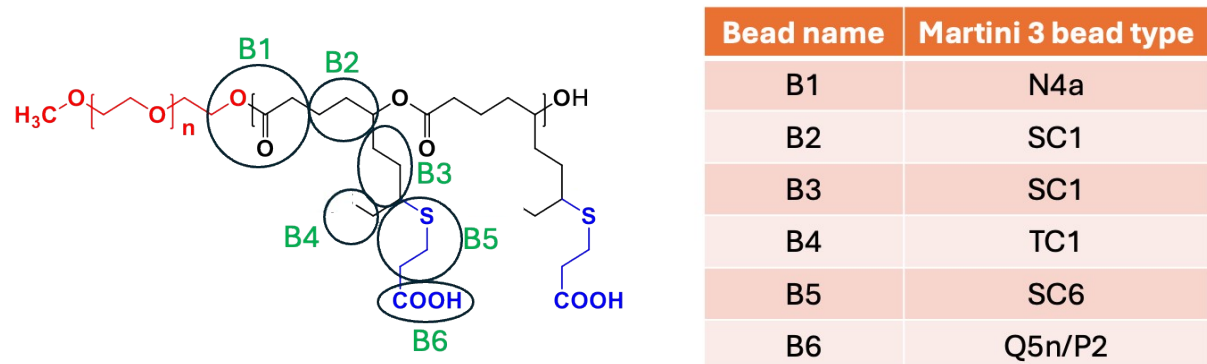
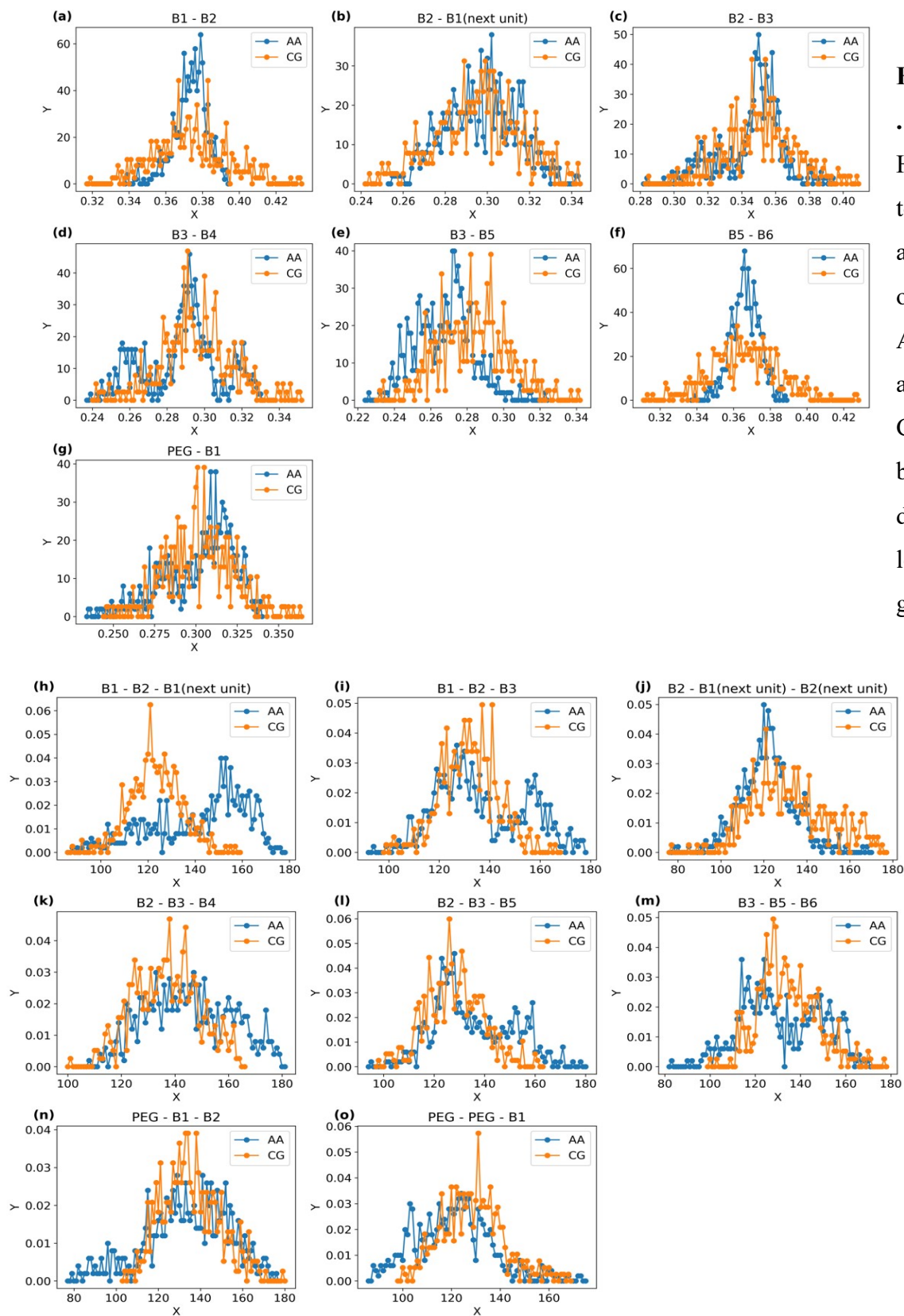


Fig. 1 Structure of the mPEG-b-PJL-COOH polymer with overlaid coarse-grained (CG) beads, where bead names are shown in green (left). The table on the right lists the Martini 3 bead types used to represent each bead in a PJL-COOH unit.

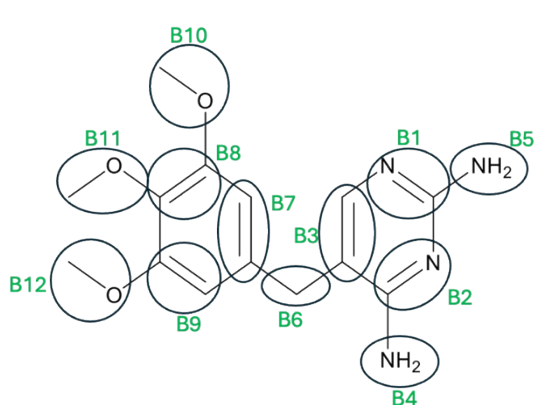
Fig . 2 His togr ams of AA and CG bon d len gth



s (a-g) and angles (h-o) among the beads representing the PJL-COOH units as shown in Fig. 1 as well as the connection between mPEG and PJL-COOH units.

The coarse-grained structure and topology of mPEG units were obtained from Polyply, a Python suite designed to facilitate the generation of Martini 3 polymer models¹¹. Based on the coarse-grained-level structural information, including bond lengths and angles, four polymer variants (P1, P2, P3, and P4) were created, containing 24, 32, 46, and 12 PJL-COOH units, respectively. All polymers contained 114 mPEG units. Additionally, P2 and P4 included 14 and 1 unit(s) of PJL (without the COOH group), respectively. Each PJL-COOH unit in P4 also featured extended aliphatic CH₂ chains adjacent to the carboxyl group, modeled following Martini 3 fatty acid parameters and connected to the PJL segment. Overall, the developed coarse-grained polymer models closely resemble the experimental structures of the four polymers used in this study.

The all-atom topology of the TMP drug molecule was parameterized using the Charmm CGenFF, with penalty scores of 13 for partial charges and 30 for torsional bonds. These values indicate reasonable analogies, which were deemed sufficient, as the purpose of the all-atom simulations was primarily to extract bond lengths and angles required for constructing the coarse-grained beads representing the TMP coarse-grained structure and topology. The coarse-grained representation of TMP units, along with comparisons of bond lengths and angles between all-atom and coarse-grained simulations, is shown in Fig. 3 and 4, respectively.



Bead name	Martini 3 bead type
B1	TN5a
B2	TN5a
B3	TC5
B4	TP3
B5	TP3
B6	TC1
B7	TC5
B8	TC5
B9	TC5
B10	TN2a
B11	TN2a
B12	TN2a

Fig. 3 Structure of the trimethoprim molecule with overlaid coarse-grained (CG) beads, where bead names are shown in green (left). The table on the right lists the Martini 3 bead types used to represent each bead for the trimethoprim molecule.

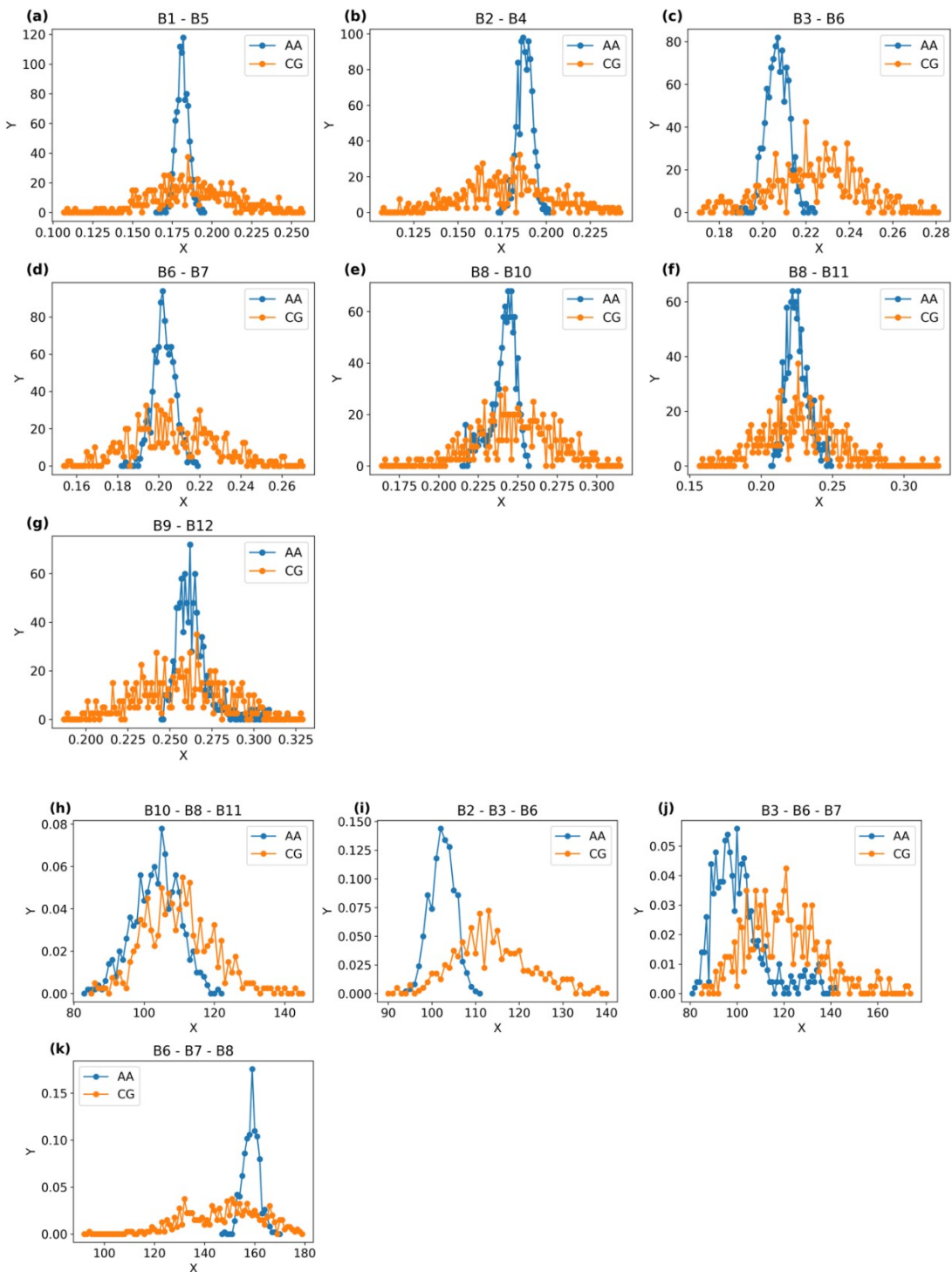


Fig. 4 Histograms of AA and CG bond lengths (a-g) and angles (h-k) among the beads representing the trimethoprim drug molecule, as shown in Fig. 3.

To investigate polymer-membrane interactions, a mixed-lipid model membrane was generated using the Charmm-GUI Membrane Builder, with Martini 3 topologies for the lipids and cholesterol^{12,13}.

4.2 Coarse-grained simulation details.

All coarse-grained simulations were performed using Gromacs 2020 and 2023¹⁴. Each system was initially energy-minimized using the steepest descent algorithm, followed by a short equilibration run of 100,000 steps with a time step of 10 fs. The last production run was performed using a 20-fs time step. The Verlet cutoff scheme was applied for both Coulombic (reaction-field) and van der Waals interactions, with a cutoff distance of 1.1 nm. Temperature coupling was maintained using the velocity-rescaling (v-rescale) thermostat with a coupling constant of 1 ps, and the system temperature was set to 303 K¹⁵.

For the production simulations, pressure was maintained using the Parrinello–Rahman barostat with a coupling constant (τ_p) of 12 ps, compressibility of 3×10^{-4} bar⁻¹, and a reference pressure of 1.0 bar¹⁶. Periodic boundary conditions were applied in all directions. Isotropic pressure coupling was used for polymer aggregation and drug-polymer interaction simulations, while semi-isotropic pressure coupling was applied for simulations involving polymer-membrane interactions with lipid bilayers.

4.3 All-atom simulation details.

All-atom simulations of a single polymer and a single drug molecule were performed using the Charmm36 force field¹⁷. Each system underwent energy minimization using the steepest descent algorithm, followed by equilibration to stabilize density and pressure. Final production runs were carried out for 500 ns using periodic boundary conditions and isotropic pressure coupling with the Parrinello–Rahman barostat. A time step of 2 fs was used, and the system temperature was maintained at 303 K using the velocity-rescale thermostat. Electrostatic interactions were calculated using the Particle Mesh Ewald (PME) method, and van der Waals interactions were evaluated using a force-switch function between 1.0 and 1.2 nm¹⁸.

4.4 Umbrella sampling (US) simulations for the TMP logP calculation.

An octanol–water system was built with two $8 \times 8 \times 8$ nm³ phases, water at the bottom and octanol on top (Fig. 5). Trimethoprim was inserted into the water phase and pulled along a reaction coordinate from the center of the water phase to the center of the octanol phase.

Umbrella sampling (US) simulations were then conducted to compute the potential of mean force (PMF) profiles for trimethoprim being pulled from the middle of the water phase to the middle of the octanol phase. A total of 81 configurations spaced 0.1 nm apart were generated along this path. Each was energy-minimized, equilibrated, and used as a starting point for 50

ns US simulations. The potential of mean force (PMF) was calculated using the weighted histogram analysis method (WHAM) via Gromacs (gmx wham)¹⁹.

From the PMF, the free energy difference (ΔG) between the water and octanol phases was found to be 8.08 kJ/mol. The logP was then calculated using:

$$\log P = \Delta G / (2.303 * R * T)$$

where, $R = 8.314 \text{ J/(mol}\cdot\text{K)}$, $T = 303 \text{ K}$. The computed LogP value was 1.4.

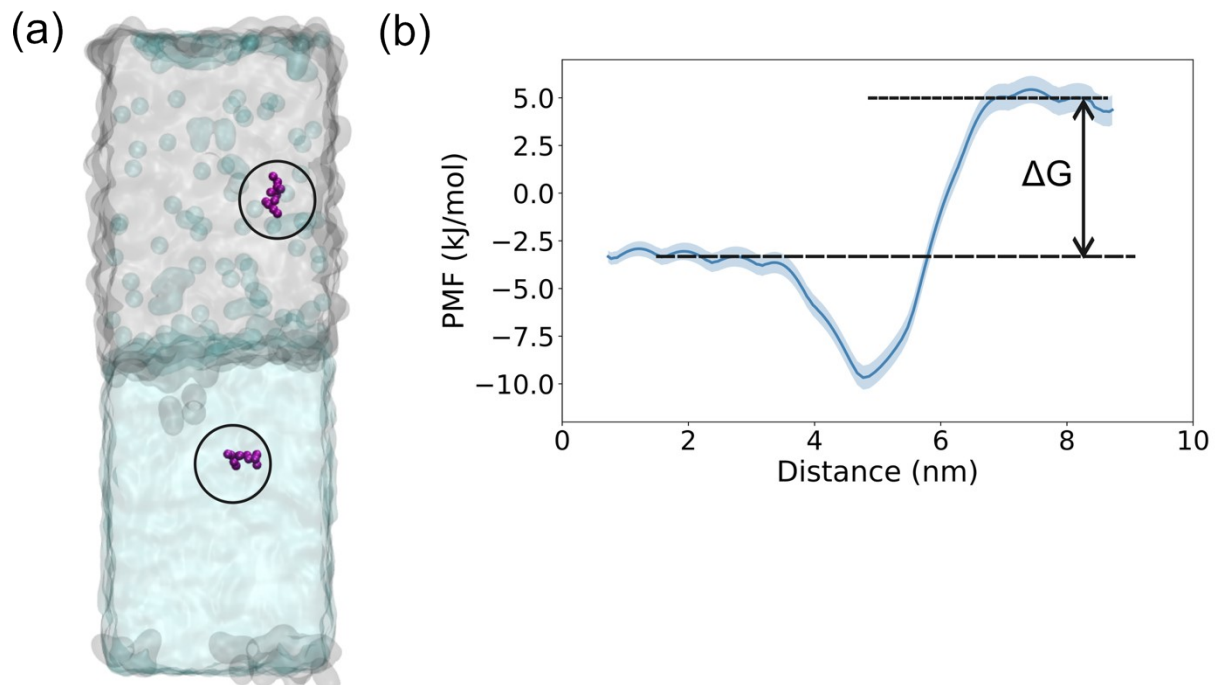


Fig. 5. LogP calculation of TMP. Snapshots of (a) trimethoprim in the water and octanol phases are shown. The gray and cyan surfaces represent the octanol and water phases, respectively. Trimethoprim is presented in van der Waals (vdW) representation and circled. (b) The free energy profiles corresponding to the pulling of trimethoprim from the octanol phase to the water phase, as illustrated in (a), is shown. The distance 0 here represents the middle of the water phase and 9.5 represents the middle of the octanol phase, respectively. The double arrow line represents the ΔG values for the free energy profiles.

5. Simulation analysis:

To calculate the number of drug molecules loaded into the polymer, a custom Python script was used with a cutoff distance of 0.5 nm²⁰. If any bead of a TMP molecule was within 0.5 nm of any bead of a polymer molecule, the drug was considered to be in contact with the polymer.

Similarly, to calculate contacts between mPEG and COOH units within the polymer, the same 0.5 nm cutoff was applied.

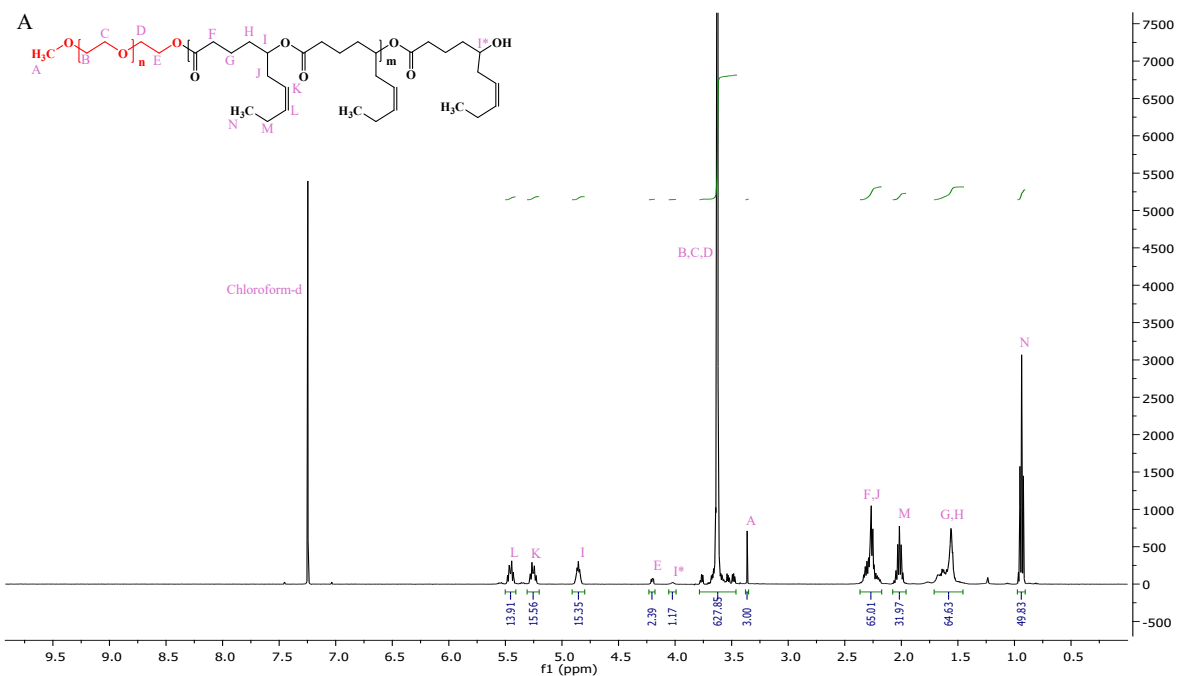
The solvent-accessible surface area (SASA) was calculated using the *gmx sasa* utility. Membrane properties, including area per lipid (APL) and membrane thickness, were calculated using the FatSLiM software²¹. The average lipid tail order parameter was calculated using the following equation:

$$P_2 = 0.5 \times (3\cos^2 \langle \theta \rangle - 1)$$

where θ is the angle between the bilayer normal and the bond vector formed by two consecutive coarse-grained beads. A value of $P_2 = 1$ indicates perfect alignment of the lipid tail with the bilayer normal, while $P_2 = 0$ corresponds to a random orientation.

Representative snapshots of the simulations were generated using VMD²².

6. Results-supporting Figures:



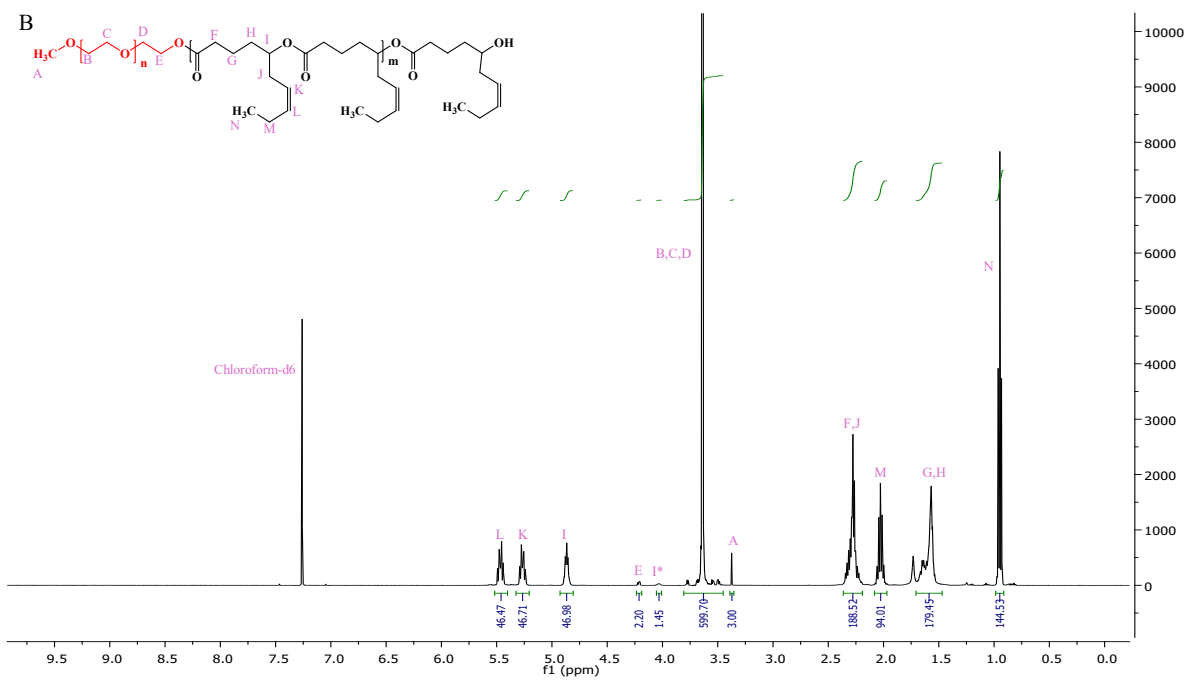


Fig. S1 (A) ^1H NMR spectra of mPEG-b-PJL (PA) and (B) mPEG-b-PJL (PB) in deuterated chloroform showed 16 (PA) and 48 (PB) repeating chain of jasmine lactone was attached to the mPEG. The mol. weight was calculated by interpreting the proton of methyl group of mPEG at 3.3ppm (A), repeating chain of jasmine lactone at 4.9ppm (I) and the proton of methyl group of jasmine lactones (N) at 0.98ppm.

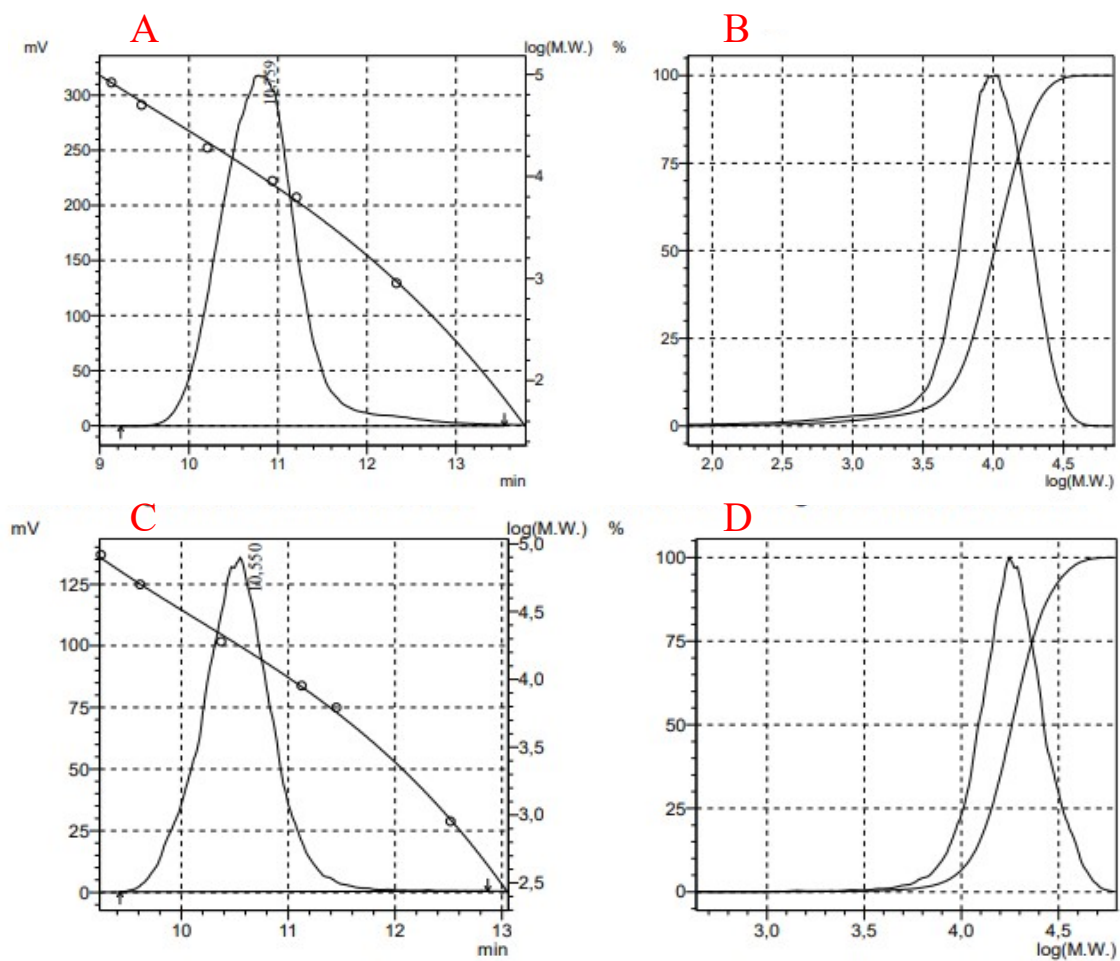


Fig. S2 High performance size exclusion chromatography (HPSEC) chromatogram & calibration curve (A, C) and molecular weight distribution curve (B, D) of the synthesized parent block co polymers, PA and PB respectively. Obtained using tetrahydrofuran (THF) as the mobile phase against polystyrene standards for molecular weight calibration.

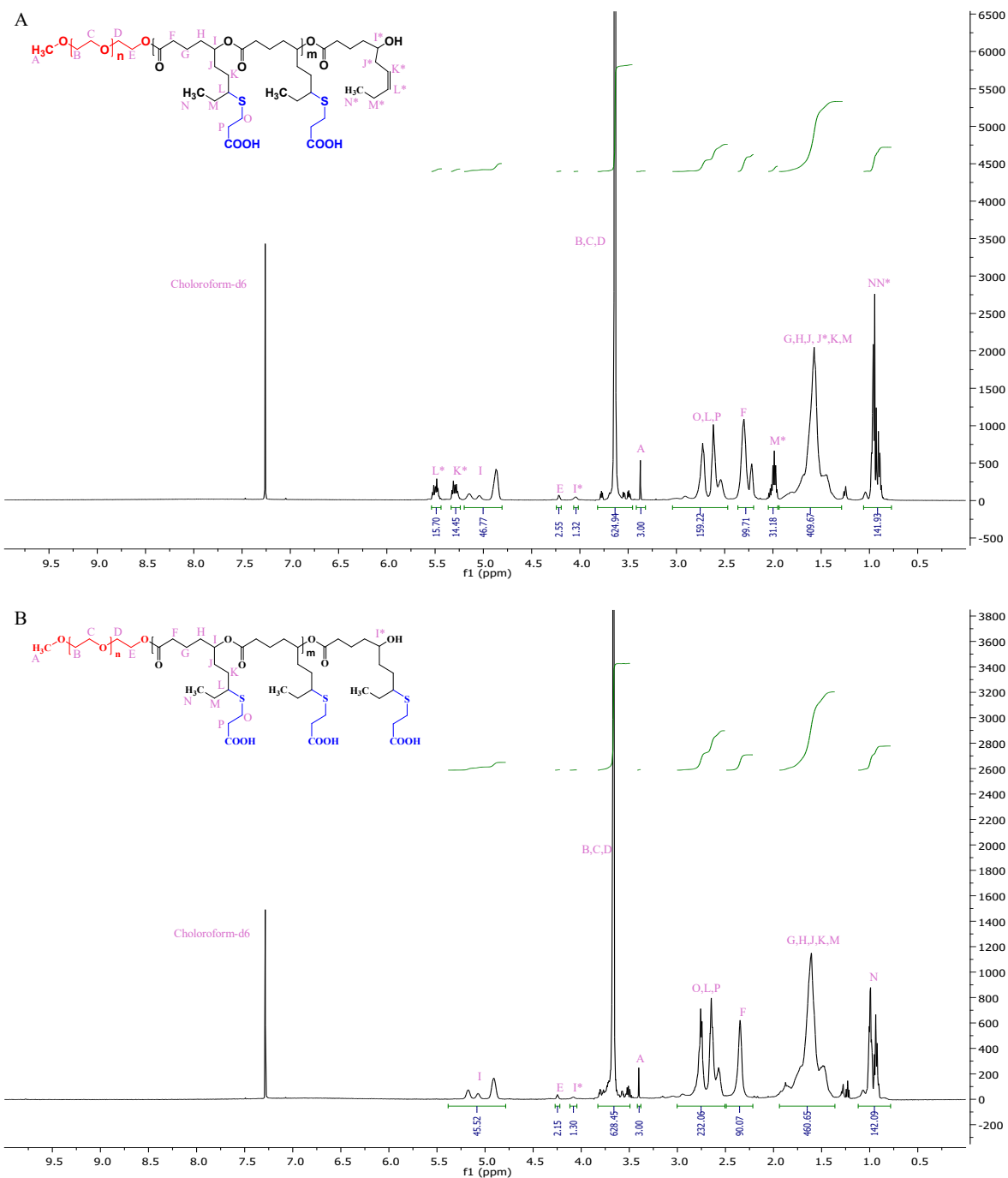


Fig. S3 (A) ^1H NMR spectra of P2 in deuterated chloroform showed presence of peak at 2.0, 5.3 and 5.5 (M*, K* and L*) suggesting that P2 still have 15 ene which confirms 70% functionalization while (B) ^1H NMR spectra of P3 in deuterated chloroform showed the disappearance of peak at 2.0, 5.3 and 5.5 ppm confirms 100% functionalization of mPEG-b-PJL to mPEG-b-PJL-COOH.

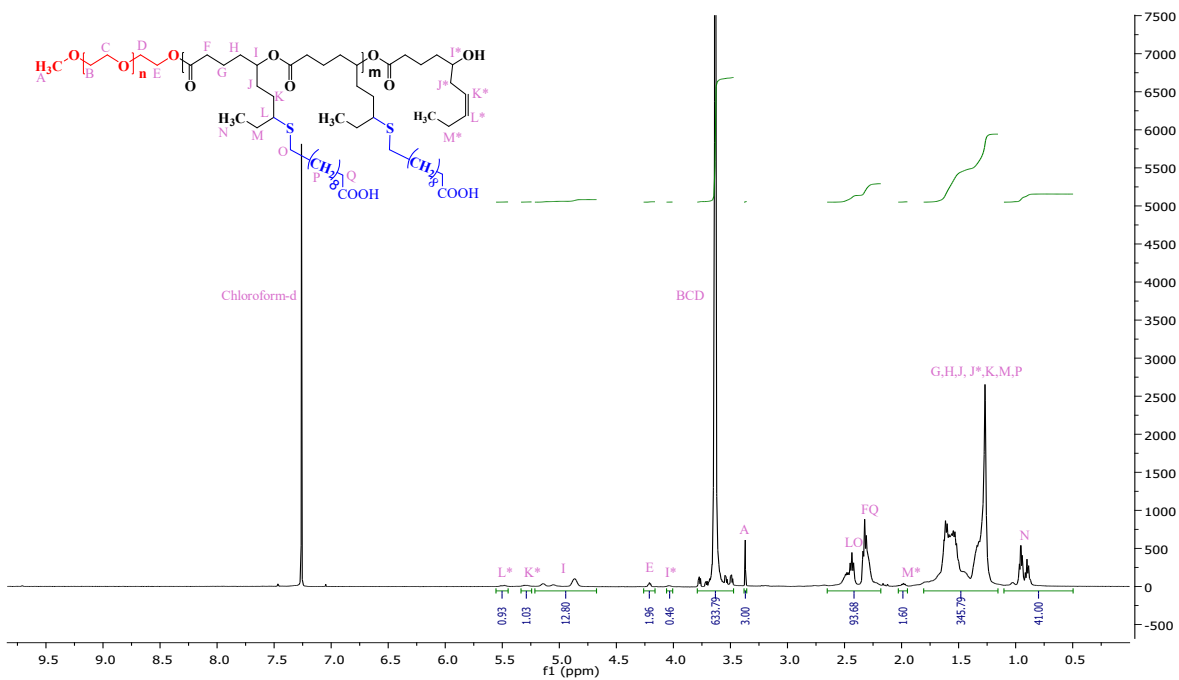


Fig. S4 ¹NMR spectra of P4 in deuterated chloroform showed presence of peak at 2.0, 5.3 and 5.5 (M*, K* and L*) suggesting that it still have 1 ene group which confirms 93% functionalization of mPEG-b-PJL to mPEG-b-PJL-COOH by 11-mercaptoundecanoic acid.

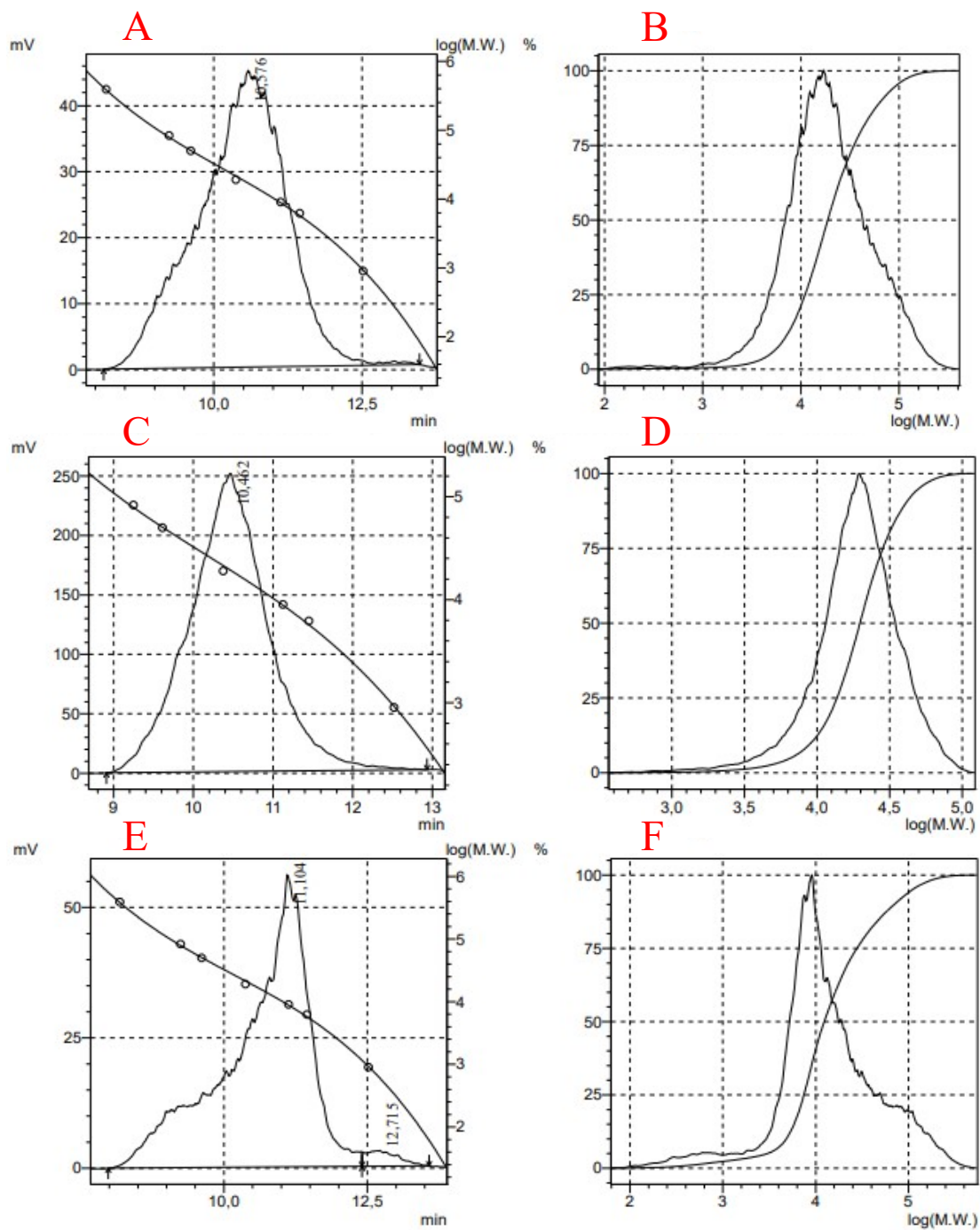


Fig. S5 High performance size exclusion chromatography (HPSEC) chromatogram presented as retention time (A, C, and E) and the molecular weight distribution curve (B, D and F) of the synthesized block co polymers, P2, P3 and P4 respectively. Tetrahydrofuran (THF) was used as the mobile phase and polystyrene standards calibration curve was used for molecular weight distribution.

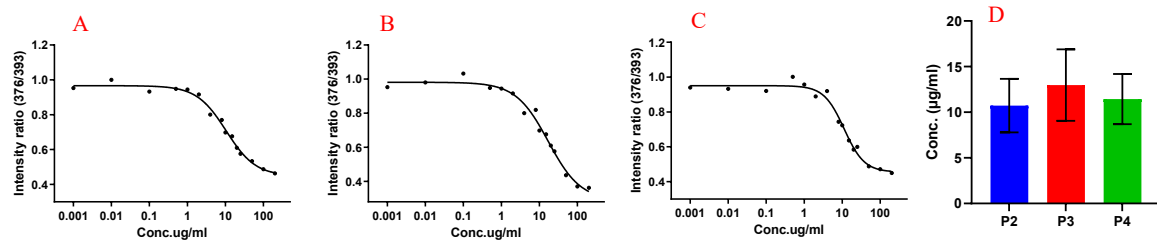


Fig. S6 Normalized pyrene intensity ($I_1:I_3$) ratio v/s log concentration (scale \log_{10}) sigmoidal graphs of the P2 (A), P3 (B), and P4 (C) to calculate CMC value (D). The inflection point (IC) of the sigmoidal curve was considered as the CMC value of the polymer.

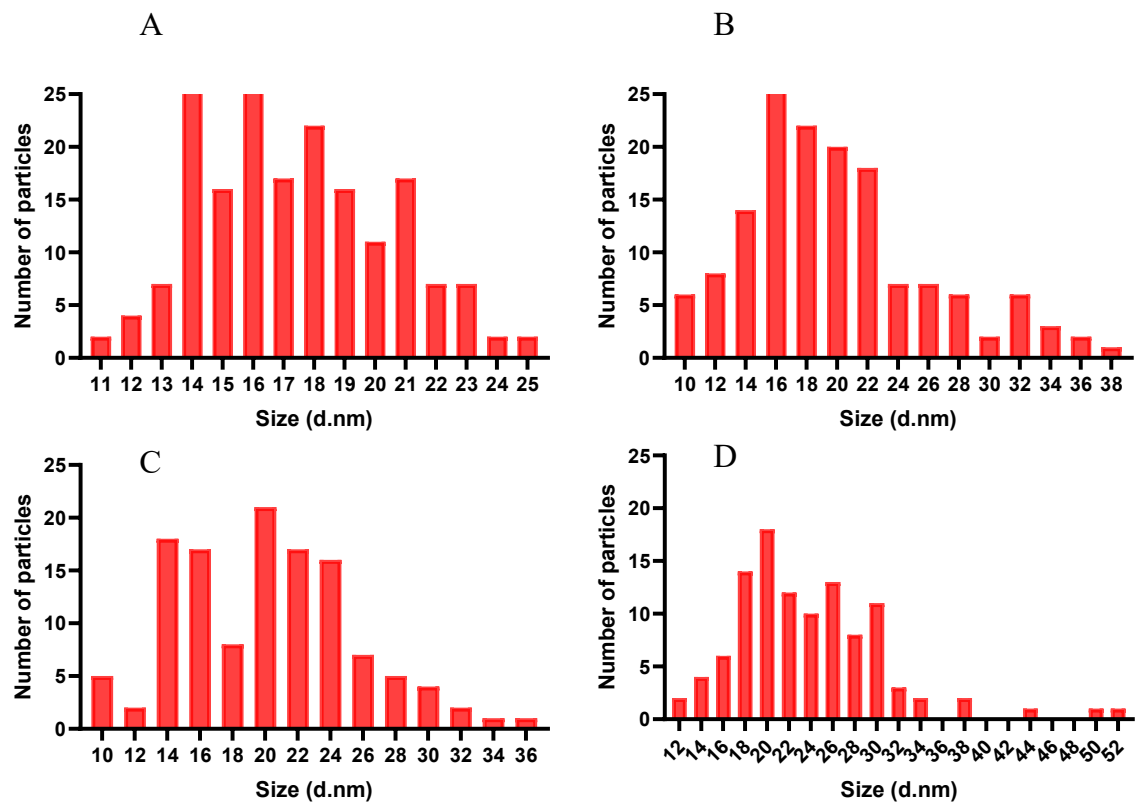


Fig. S7 Histogram of the transmission electron microscopy (TEM) images of TMP loaded P1-M, P2-M, P3-M, and P4-M using image J software.

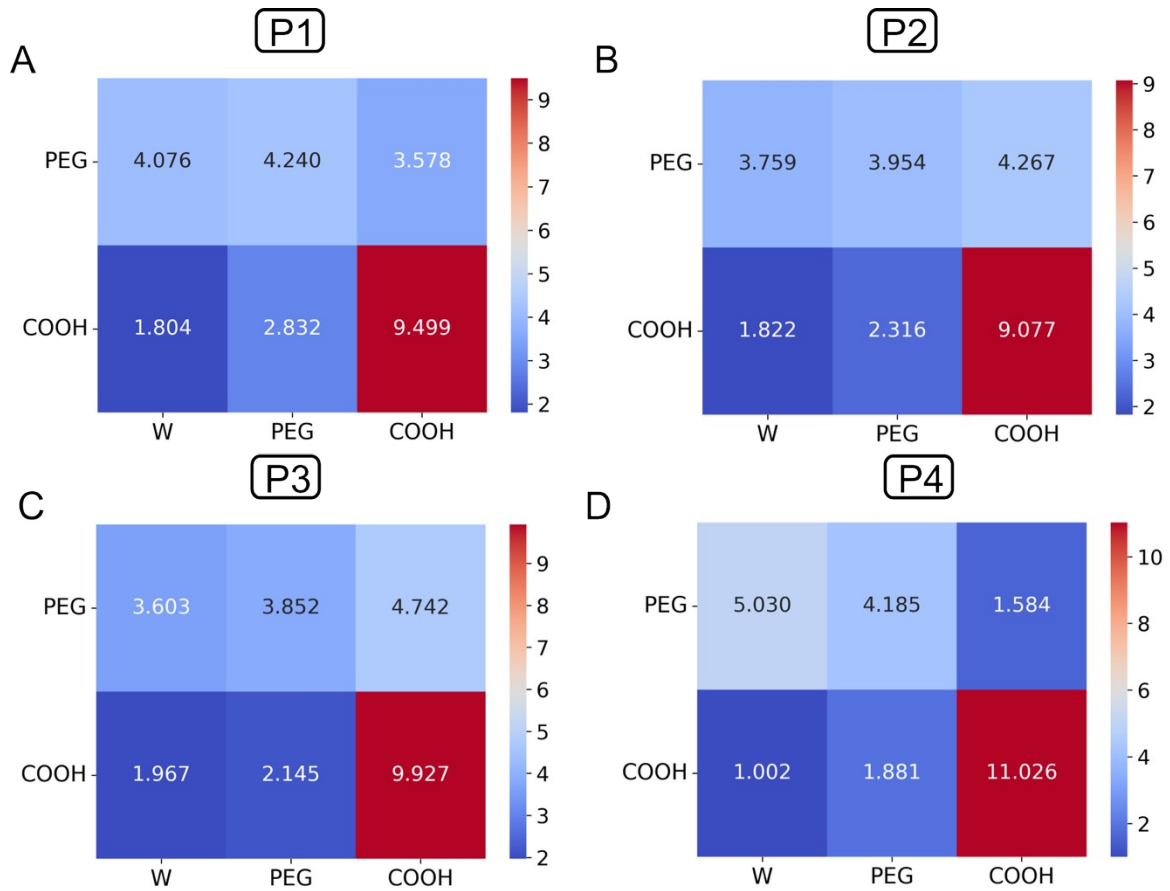


Fig. S8 Average number of contacts between the PEG (mPEG) and COOH units of the polymers—both among themselves and with surrounding water beads—calculated over the last 200 ns of the simulation for the four polymers: P1, P2, P3, and P4. Contacts involving mPEG (mPEG–W, mPEG–mPEG, and mPEG–COOH; shown in the first row of each Fig.) are normalized by the number of mPEG beads in the system. Likewise, contacts involving COOH (COOH–W, COOH–mPEG, and COOH–COOH; shown in the second row) are normalized by the number of COOH beads.

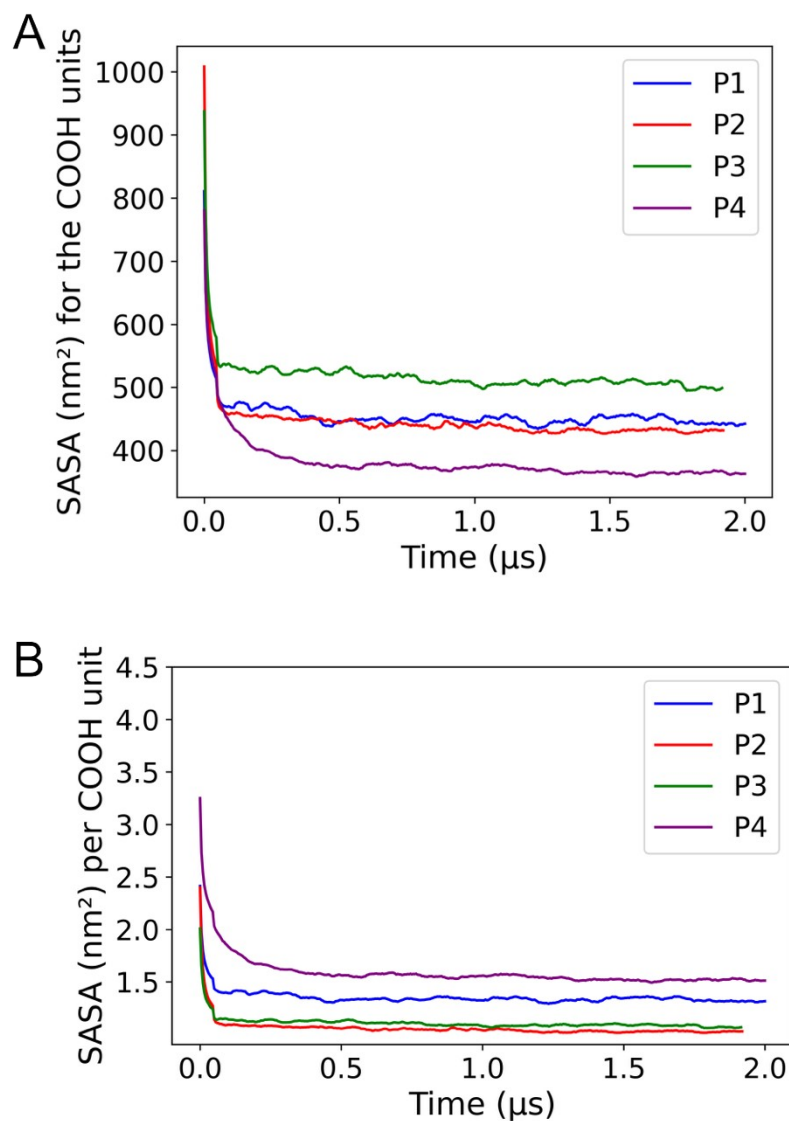


Fig. S9 Evolution of the hydrophobic solvent-accessible surface area (SASA) during the simulations, shown for all COOH units combined (A) and normalized per COOH unit (B).

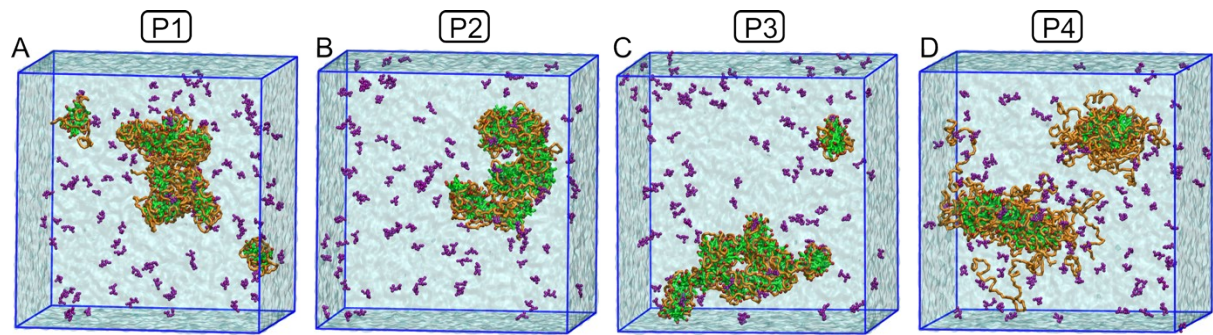


Fig. S10 Simulations of drug–polymer interactions. Panels A–D show initial snapshots of drug-loaded polymers for the four polymers: P1, P2, P3, and P4, respectively. Color scheme: mPEG and COOH units of the polymers are shown in orange and green licorice representations, respectively. Charged carboxylate beads are shown in red. Water is rendered with a cyan surface representation. TMP molecules are represented as purple beads.

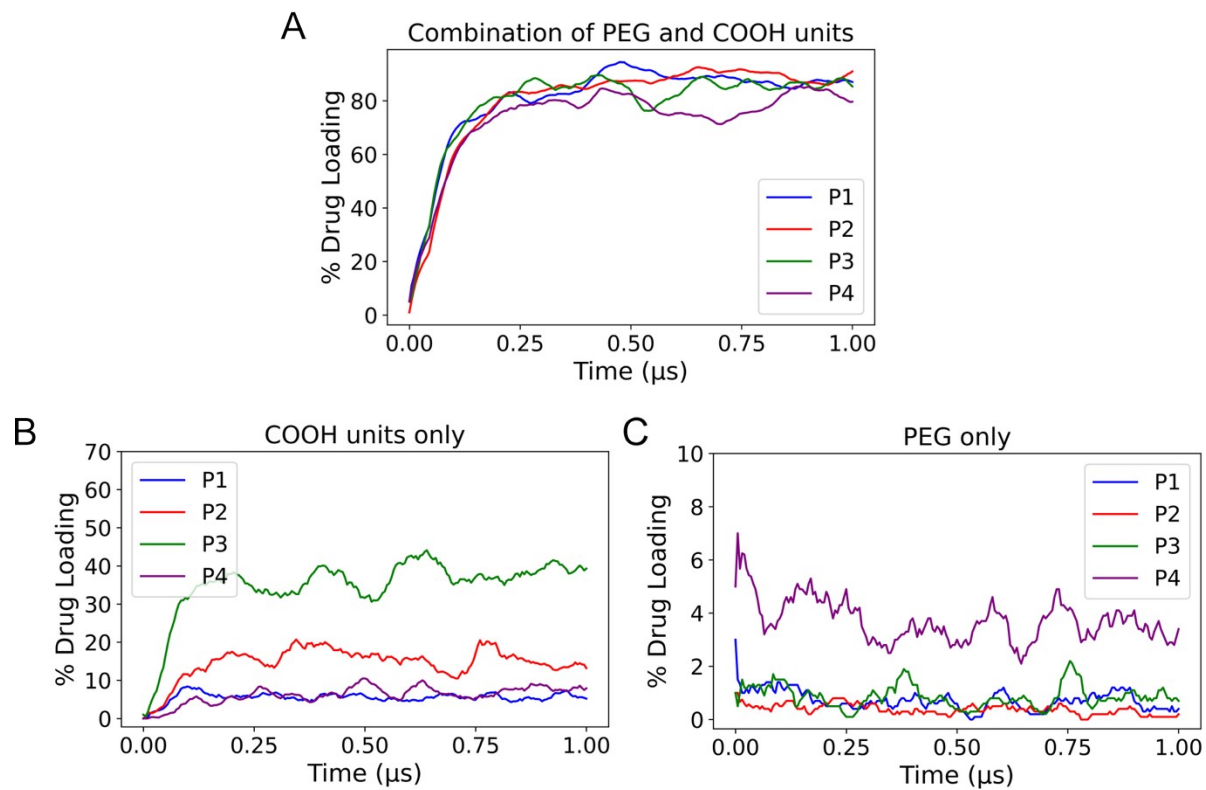


Fig. S11 Evolution of % Drug Loading during the simulations: (A) combined contribution of mPEG and COOH units, (B) contribution from COOH units alone, and (C) contribution from mPEG units alone.

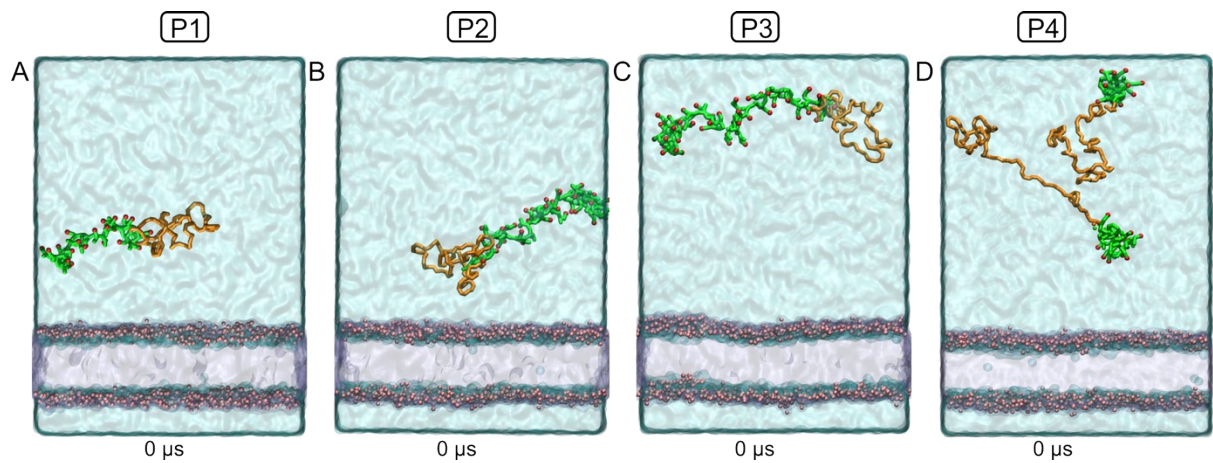


Fig. S12 Initial snapshots from polymer micelle–membrane interaction simulations. Panels A–D show the initial configurations for polymers P1, P2, P3, and P4, respectively. Color scheme: mPEG and COOH units of the polymers are shown in orange and green licorice representations, respectively; charged carboxylate beads are in red. Water is shown as a cyan surface, lipid headgroups as pink beads, and lipid tails as an ice-blue surface.

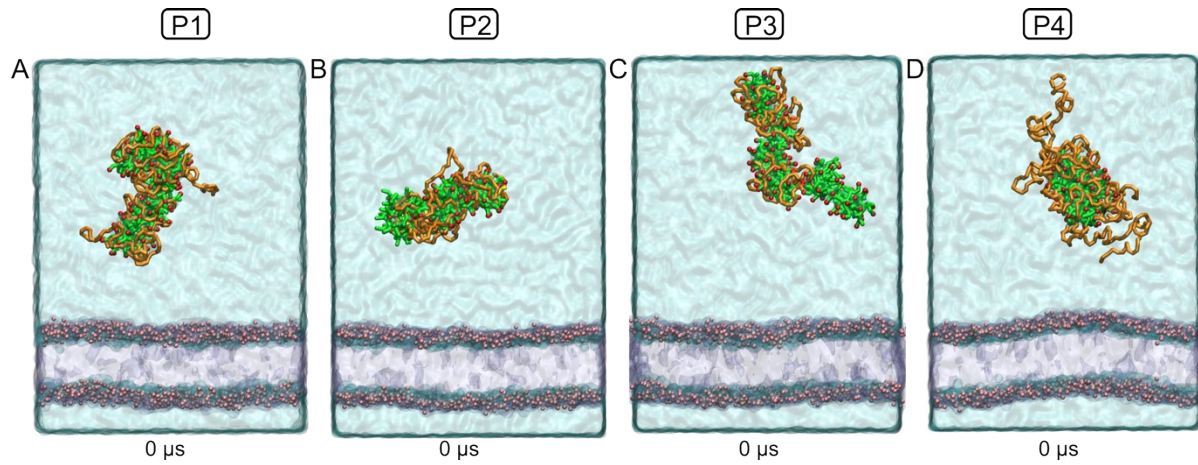


Fig. S13 Initial snapshots from polymer micelle–membrane interaction simulations. Panels A–D show the initial configurations for polymers P1, P2, P3, and P4, respectively. Color scheme: mPEG and COOH units of the polymers are shown in orange and green licorice representations, respectively; charged carboxylate beads are in red. Water is shown as a cyan surface, lipid headgroups as pink beads, and lipid tails as an ice-blue surface.

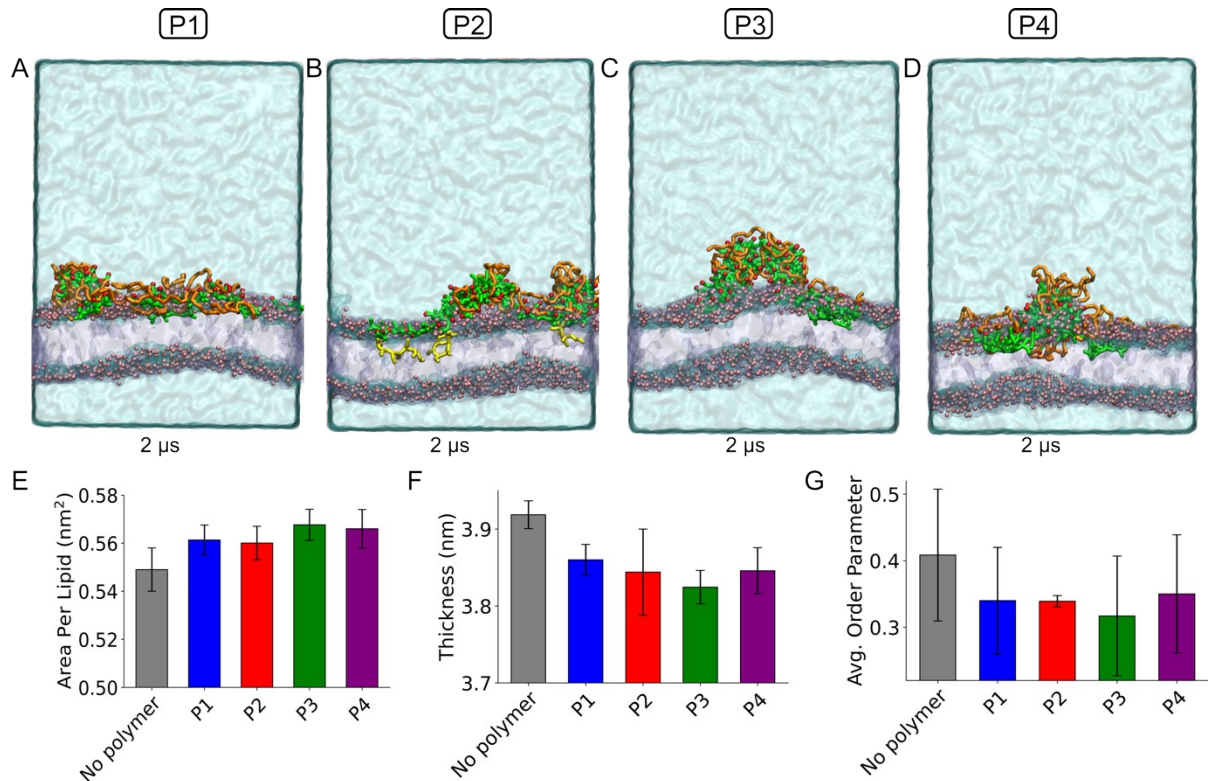


Fig. S14 Final snapshots and membrane structural properties from polymer micelle–membrane interaction simulations. Panels A–D show the final configurations for polymers P1, P2, P3, and P4, respectively. Panels E–G present the average values of membrane area per lipid (E), thickness (F), and lipid tail order parameter (G) over the last 500 ns of the simulations, with and without polymers. Color scheme: mPEG and COOH units of the polymers are shown in orange and green licorice representations, respectively; charged carboxylate beads are in red. Water is shown as a cyan surface, lipid head groups as pink beads, and lipid tails as an ice-blue surface.

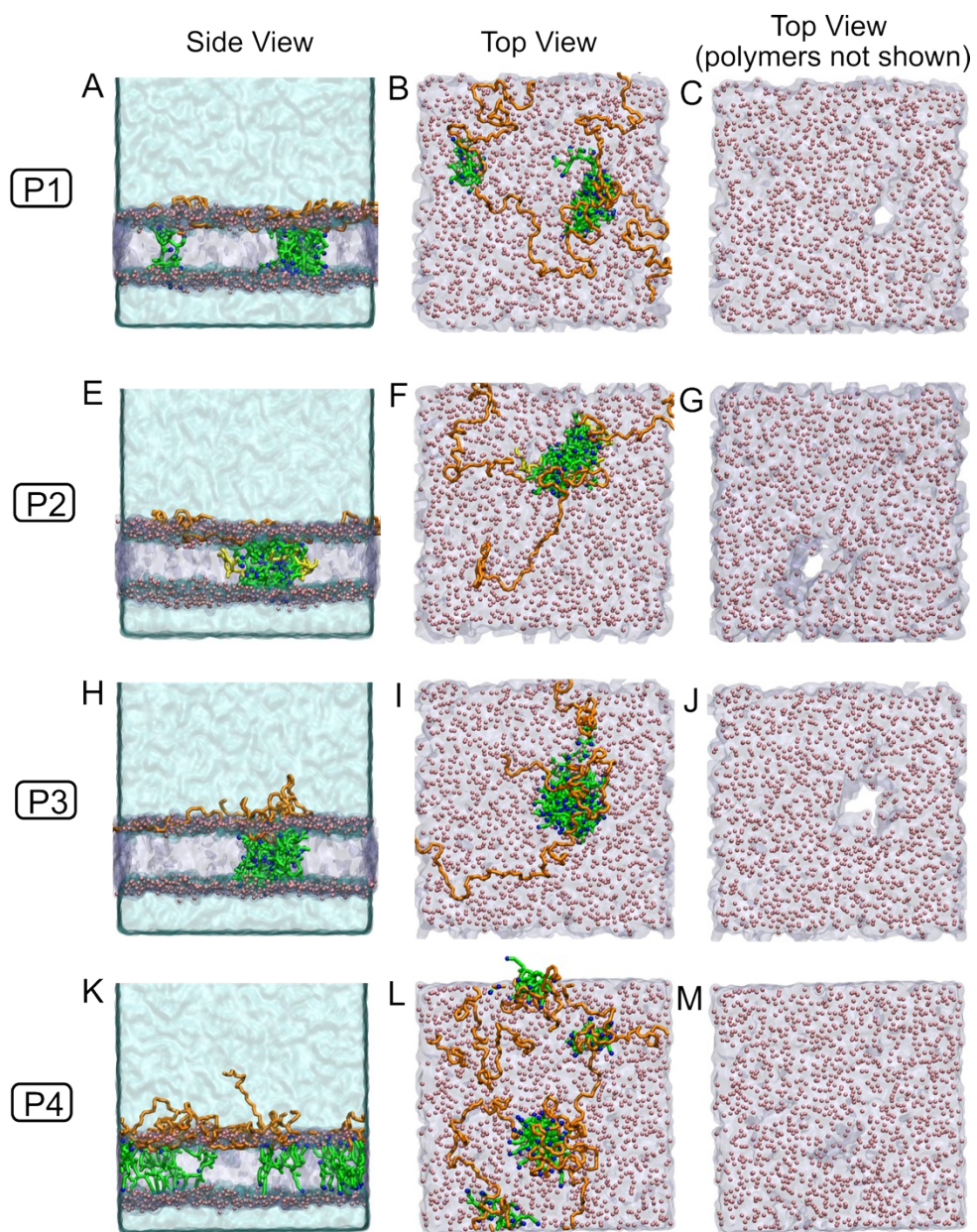


Fig. S15 Snapshots from simulations of polymer micelles containing neutral COOH units interacting with a membrane. Panels A, E, H, and K show the side views of the final configurations at 3 microseconds for the four polymers: P1, P2, P3, and P4, respectively. Panels B, F, I, and L present the corresponding top views, while panels C, G, J, and M show the top views with membrane-embedded polymer molecules hidden for clarity. Color scheme: mPEG and COOH units of the polymers are shown in orange and green licorice representations, respectively. Neutral carboxylic acid beads are depicted in blue. Water is rendered as a cyan surface. Membrane lipid headgroups are shown as pink beads, while the lipid tails are represented using an ice-blue surface rendering.

Table S1 The detailed simulation system descriptions.

#	Polymer	# of molecules	# of COOH units	Equivalent concentration	Simulation time (μs)	Box size (nm×nm ×nm)
Polymer aggregation simulations						
1	P1	14	336	~20 mg	2	25×25×25
2	P2	10	320	~20 mg	2	25×25×25
3	P3	8	368	~20 mg	2	25×25×25
4	P4	18	16	~20 mg	2	25×25×25
Drug-Polymer Interaction simulations						
1	P1	14 P1, 98 drug	336	~20 mg P1, ~3 mg drug	1	25×25×25
2	P2	10 P2, 98 drug	320	~20 mg P2, ~3 mg drug	1	25×25×25
3	P3	8 P3, 98 drug	368	~20 mg P3, ~3 mg drug	1	25×25×25
4	P4	18 P4, 98 drug	216	~20 mg P4, ~3 mg drug	1	25×25×25
Membrane-Polymer monomer Interaction simulations						
1	P1 with charged COOH units	1 P1, 450 POPC, 220 POPE, 100 POPS, 240 CHOL	24	N/A	1	20×20×29
2	P1 with neutral COOH units					
3	P2 with charged COOH units	1 P2, 450 POPC, 220 POPE, 100 POPS, 240 CHOL	32	N/A	1	20×20×29
4	P2 with neutral COOH units					
5	P3 with charged COOH units	1 P3, 450 POPC, 220 POPE, 100 POPS, 240 CHOL	46	N/A	1	20×20×29
6	P3 with neutral COOH units					
7	P4 with charged COOH units	2 P4, 450 POPC, 220 POPE, 100 POPS, 240 CHOL	24	N/A	1	20×20×29
8	P4 with neutral COOH units					
Membrane-Polymer micelle Interaction simulations						
1	P1 with charged COOH units	4 P1, 450 POPC, 220 POPE, 100 POPS, 240 CHOL	96	~10 mg P1	1	20×20×29
2	P1 with neutral COOH units					
3	P2 with charged COOH units	3 P2, 450 POPC, 220 POPE, 100 POPS, 240 CHOL	96	~10 mg P2	1	20×20×29
4	P2 with neutral COOH units					
5	P3 with charged COOH units	3 P3, 450 POPC, 220 POPE, 100 POPS, 240 CHOL	138	~10 mg P3	1	20×20×29
6	P3 with neutral COOH units					
7	P4 with charged COOH units	6 P4, 450 POPC, 220 POPE, 100 POPS, 240 CHOL	72	~10 mg P4	1	20×20×29
8	P4 with neutral COOH units					

7. References:

1. Bansal KK, Özliseli E, Rosling A, Rosenholm JM. Synthesis and Evaluation of Novel Functional Polymers Derived from Renewable Jasmine Lactone for Stimuli-Responsive Drug Delivery. *Advanced Functional Materials*. 2021;31(33):2101998.
2. Moghrabi FS, Fadda HM. Drug Physicochemical Properties and Capsule Fill Determine Extent of Premature Gastric Release from Enteric Capsules. *Pharmaceutics*. 2022 Nov 18;14(11):2505.
3. Verma J, Kumar V, Wilen CE, Rosenholm JM, Bansal KK. Reactive Oxygen Species-Regulated Conjugates Based on Poly(jasmine) Lactone for Simultaneous Delivery of Doxorubicin and Docetaxel. *Pharmaceutics*. 2024 Sept;16(9):1164.
4. Maru S, Verma J, Wilen CE, Rosenholm JM, Bansal KK. Attenuation of celecoxib cardiac toxicity using Poly(δ -decalactone) based nanoemulsion via oral route. *Eur J Pharm Sci*. 2023 Nov 1;190:106585.
5. Bansal KK, Özliseli E, Saraogi GK, Rosenholm JM. Assessment of Intracellular Delivery Potential of Novel Sustainable Poly(δ -decalactone)-Based Micelles. *Pharmaceutics*. 2020 Aug 2;12(8):726.
6. Bansal KK, Gupta J, Rosling A, Rosenholm JM. Renewable poly(δ -decalactone) based block copolymer micelles as drug delivery vehicle: *in vitro* and *in vivo* evaluation. *Saudi Pharmaceutical Journal*. 2018 Mar 1;26(3):358–68.
7. Kakde D, Taresco V, Bansal KK, Magennis EP, Howdle SM, Mantovani G, et al. Amphiphilic block copolymers from a renewable ϵ -decalactone monomer: prediction and characterization of micellar core effects on drug encapsulation and release. *J Mater Chem B*. 2016 Nov 9;4(44):7119–29.
8. Souza PCT, Alessandri R, Barnoud J, Thallmair S, Faustino I, Grünwald F, et al. Martini 3: a general purpose force field for coarse-grained molecular dynamics. *Nat Methods*. 2021 Apr;18(4):382–8.
9. Choi YK, Park SJ, Park S, Kim S, Kern NR, Lee J, et al. CHARMM-GUI Polymer Builder for Modeling and Simulation of Synthetic Polymers. *J Chem Theory Comput*. 2021 Apr 13;17(4):2431–43.
10. Vanommeslaeghe K, MacKerell ADJr. Automation of the CHARMM General Force Field (CGenFF) I: Bond Perception and Atom Typing. *J Chem Inf Model*. 2012 Dec 21;52(12):3144–54.
11. Grünwald F, Alessandri R, Kroon PC, Monticelli L, Souza PCT, Marrink SJ. Polyply; a python suite for facilitating simulations of macromolecules and nanomaterials. *Nat Commun*. 2022 Jan 10;13(1):68.

12. Wu EL, Cheng X, Jo S, Rui H, Song KC, Dávila-Contreras EM, et al. CHARMM-GUI Membrane Builder toward realistic biological membrane simulations. *Journal of Computational Chemistry*. 2014;35(27):1997–2004.
13. Borges-Araújo L, Borges-Araújo AC, Ozturk TN, Ramirez-Echemendia DP, Fábián B, Carpenter TS, et al. Martini 3 Coarse-Grained Force Field for Cholesterol. *J Chem Theory Comput*. 2023 Oct 24;19(20):7387–404.
14. Abraham MJ, Murtola T, Schulz R, Páll S, Smith JC, Hess B, et al. GROMACS: High performance molecular simulations through multi-level parallelism from laptops to supercomputers. *SoftwareX*. 2015 Sept 1;1–2:19–25.
15. Bussi G, Donadio D, Parrinello M. Canonical sampling through velocity rescaling. *J Chem Phys*. 2007 Jan 3;126(1):014101.
16. Parrinello M, Rahman A. Polymorphic transitions in single crystals: A new molecular dynamics method. *J Appl Phys*. 1981 Dec 1;52(12):7182–90.
17. Vanommeslaeghe K, Hatcher E, Acharya C, Kundu S, Zhong S, Shim J, et al. CHARMM general force field: A force field for drug-like molecules compatible with the CHARMM all-atom additive biological force fields. *Journal of Computational Chemistry*. 2010;31(4):671–90.
18. Darden T, York D, Pedersen L. Particle mesh Ewald: An $N \cdot \log(N)$ method for Ewald sums in large systems. *J Chem Phys*. 1993 June 15;98(12):10089–92.
19. Hub JS, de Groot BL, van der Spoel D. g_wham—A Free Weighted Histogram Analysis Implementation Including Robust Error and Autocorrelation Estimates. *J Chem Theory Comput*. 2010 Dec 14;6(12):3713–20.
20. Hossain S, Parrow A, Kabedev A, Kneisl RC, Leng Y, Larsson P. Explicit-pH Coarse-Grained Molecular Dynamics Simulations Enable Insights into Restructuring of Intestinal Colloidal Aggregates with Permeation Enhancers. *Processes*. 2022 Jan;10(1):29.
21. Buchoux S. FATSLiM: a fast and robust software to analyze MD simulations of membranes. *Bioinformatics*. 2017 Jan 1;33(1):133–4.
22. Humphrey W, Dalke A, Schulten K. VMD: visual molecular dynamics. *J Mol Graph*. 1996 Feb;14(1):33–8, 27–8.